Biogeosciences Discuss., 6, 163–196, 2009
www.biogeosciences-discuss.net/6/163/2009/

Biogeosciences Discussions

Biogeosciences Discussions is the access reviewed discussion forum of *Biogeosciences*

Advection of NH_3 over a pasture field, and its effect on gradient flux measurements

B. Loubet[1], C. Milford[2,*], A. Hensen[3], U. Daemmgen[4], J.-W. Erisman[3], P. Cellier[1], and M. A. Sutton[2]

[1]Institut National de la Recherche Agronomique (INRA), UMR Environnement et Grandes Cultures, Thiverval-Grignon, 78850, France
[2]Centre for Ecology and Hydrology (Edinburgh Research Station), Bush Estate, Penicuik, Midlothian, EH26 0QB, UK
[3]Energy research Centre of the Netherlands (ECN), Postbus 1, 1755 ZG Petten, The Netherlands
[4]Institut fur Agrarokologie, Bundesforschungsanstalt fur Landwirtschaft (FAL), Bundesallee 50, 38116 Braunschweig, Germany
[*]now at: Institute of Earth Sciences "Jaume Almera", CSIC, Lluis Solé i Sabarís, 08028, Barcelona, Spain

Received: 7 October 2008 – Accepted: 22 October 2008 – Published: 6 January 2009

Correspondence to: B. Loubet (loubet@grignon.inra.fr)

Published by Copernicus Publications on behalf of the European Geosciences Union.

Abstract

Deposition of atmospheric ammonia (NH_3) to semi-natural ecosystems leads to serious adverse effects, such as acidification and eutrophication. A step in this quantification is the measurement of NH_3 fluxes over semi-natural and agricultural land. However, measurement of NH_3 fluxes over vegetation in the vicinity of strong NH_3 sources is difficult, since NH_3 emissions are highly heterogeneous. Indeed, under such conditions, local advection errors may alter the measured fluxes. In this study, local advection errors ($\Delta F_{z,\mathrm{adv}}$) were estimated over a 14 ha grassland field, which was successively cut and fertilised, as part of the GRAMINAE integrated Braunschweig experiment. The magnitude of $\Delta F_{z,\mathrm{adv}}$ was determined up to 810 m downwind from farm buildings emitting between 6 and 12 kg NH_3 day^{-1}. The GRAMINAE experiment provided a unique opportunity to compare two methods of estimating $\Delta F_{z,\mathrm{adv}}$: (1) based on direct measurements of horizontal concentration gradients, and (2) based on inverse dispersion modelling.

Two sources of local advection were clearly identified: the farm NH_3 emissions leading to positive $\Delta F_{z,\mathrm{adv}}$, and field NH_3 emissions, after cutting and fertilisation, which led to a negative $\Delta F_{z,\mathrm{adv}}$. The local advection flux from the farm was in the range 0 to 27 ng m^{-2} s^{-1} NH_3 at 610 m from the farm, whereas $\Delta F_{z,\mathrm{adv}}$ due to field emission was proportional to the local flux, and ranged between −209 and 13 ng m^{-2} s^{-1} NH_3. The local advection flux $\Delta F_{z,\mathrm{adv}}$ was either positive or negative depending on the magnitude of these two contributions. The modelled and measured advection errors agreed well, provided the modelled $\Delta F_{z,\mathrm{adv}}$ was estimated at 2 m height. This study constitutes the first attempt to validate the inverse modelling approach to determine advection errors for NH_3. The measured advection errors, relative to the vertical flux at 1 m height, were 121% on average, before the field was cut (when downwind of the farm), and less than 7% when the field was fertilised.

1 Introduction

Ammonia has long been used by humans for manufacture and fertilization (Sutton et al., 2008). Deposition of atmospheric ammonia (NH_3) may lead to severe adverse effects on sensitive ecosystems, such as acidification and eutrophication (Fangmeier et al., 1994; Krupa, 2003), as well as to agricultural land that is more exposed to larger NH_3 concentrations (van der Eerden et al., 1998). Ammonia emissions mainly originate from farm livestock and fields spread manure, as well as fields following the application of mineral fertilisers (Bouwman et al., 1997; Sommer et al., 2003). Estimating the net NH_3 emissions from farms and their surrounding fields, which might act as sources or sinks depending on season and management (e.g., Milford et al., 2001a), is essential to quantify the net input of NH_3 from agriculture to the atmosphere on a regional scale. Hence, measuring the NH_3 flux with vegetation is necessary to (i) assess pollution impacts to sensitive ecosystems, as well as (ii) quantify NH_3 emissions and deposition to agricultural fields. The most realistic way of measuring NH_3 flux between the atmosphere and the surface are the micrometeorological gradient method (Erisman and Wyers, 1993; Fowler et al., 2001; Sutton et al., 1993, 2001; Wichink Kruit et al., 2007), Bowen ratio method (Walker et al., 2006), Relaxed Eddy Accumulation (REA) methods (Kaimal and Finnigan, 1994; Hensen et al., 2008), as well as eddy-covariance with tunable diode laser (Withehead et al., 2008). All these methods rely on the assumption of non-divergence of the vertical flux (e.g., Fowler and Duyzer, 1989; Lee et al., 2004; Foken et al., 2006). Such divergence might exist in conditions of either (1) unsteadiness (temporal variation) of the flow or the sources/sinks, (2) chemical reactions consuming or releasing NH_3 in the atmosphere, or (3) heterogeneity in the spatial distribution of the sources and sinks, either of momentum or NH_3. Agricultural landscapes exhibit many of the undesired criteria: large NH_3 sources, such as animal housing, grazing cattle or fields after manure or fertiliser application, are often in close juxtaposition to natural or agricultural ecosystems acting as NH_3 receptors (Sutton et al., 1998; Hertel et al., 2006; Walker et al., 2008). The short lifetime of NH_3 in the atmosphere leads to rapid chemical reactions (Brost et al., 1988; Nemitz et al., 1997, 2000; Nemitz and Sutton, 2004). As a consequence, measurements of NH_3 ground fluxes with micrometeorological methods may often be liable to errors due to divergence of the vertical flux, linked with the heterogeneity of the source and sinks, as well as chemical reactions (Nemitz and Sutton, 2004), leading to local advection (Loubet et al., 2001, 2006; Milford et al., 2001b).

In the present study, the local advection fluxes were estimated as part of the GRAMINAE Integrated Experiment (Sutton et al., 2008) over an experimental field of about 600 m×300 m, located 230 m downwind of a set of farm buildings (Fig. 1) over a month period, during which the field was cut and fertilized. There were two sources of local advection fluxes: the farm buildings and the field itself (Fig. 1). This paper addresses the issue of advection using both measurements and modelling techniques. The latter is based on the inversion of a simplified dispersion-exchange model (Loubet et al., 2001) to fit measured concentration profiles at a known distance from a delimited source, and this technique also provides an alternative means to quantify net surface exchange fluxes in a similar manner as Wilson et al. (1983).

2 Estimation of advection errors

2.1 Theoretical background

For simplicity, only vertical- and along-wind directions are considered, in which case, the conservation equation for NH_3 in the atmospheric surface layer becomes (Fowler and Duyzer, 1989):

$$\frac{\partial F_z}{\partial z} = \underset{\mathrm{I}}{\frac{\partial \chi_a}{\partial t}} - \underset{\mathrm{II}}{\frac{\partial F_x}{\partial x}} - \underset{\mathrm{III}}{Q_{\mathrm{chem}}} \tag{1}$$

Where z is the height above the displacement height d, t is time, x is downwind distance, χ_a is the NH_3 concentration, F_z and F_x are the vertical and horizontal components of the NH_3 flux, respectively, and Q_{chem} is the net chemical source or sink density. The left-hand term, $\partial F_z/\partial z$, is the vertical flux divergence, (I) is the storage term, (II) is the horizontal flux divergence, and (III) is the chemical source/sink term. For NH_3, which is rapidly exchanged with the surface, the storage term due to $\partial \chi_a/\partial t$ is usually negligible (e.g. Sutton et al., 1993). In situations with sufficient concentrations, the perturbation of the NH_3-HNO_3-NH_4NO_3 and NH_3-HCl-NH_4Cl *equilibria* due to fluxes at the surface can lead to a chemical production/consumption term Q_{chem} (Nemitz et al., 2008). This effect may potentially lead to errors of the order of 30% of F_z (Nemitz et al., 1997). Assuming that horizontal diffusion can be neglected compared to horizontal advection, which is a reasonable assumption above short vegetation (e.g., Leuning et al., 1985), F_x can be expressed as: $F_x(x,z)=u(z)\chi_a(x,z)$, where u is the mean wind speed. The term (II) in Eq. (1) can then be integrated to get an expression of the vertical flux difference due to local advection $\Delta F_{z,\mathrm{adv}}(x,z)$, at location x and height z (named local advection flux in the following) :

$$\Delta F_{z,\mathrm{adv}}(x,z) = F_z(x,z) - F_z(x,z_0) = -\int_{z_0}^{z} u(z)\frac{\partial \chi_a(x,z)}{\partial x}\,dz \tag{2}$$

where F_z is the vertical flux, z_0 is the roughness length, and $F_z(x,z_0)$ is the flux at the surface, which is what is seek in measurements. According to Eq. (2), a negative horizontal gradient of concentration (concentration decreasing with x) leads to a positive local advection flux, which corresponds to a situation downwind from a source and above a sink. On the contrary, a positive horizontal gradient of concentration leads to negative local advection fluxes, which corresponds to what would be observed above a source. Equation (2) also shows that if $\Delta F_{z,\text{adv}}$ is positive, F_Z is larger than the flux at the surface, hence measurements at a given height are "biased toward emission". On the contrary, a negative $\Delta F_{z,\text{adv}}$ means a "bias toward deposition". The following sections detail how the vertical flux divergence is inferred from the horizontal concentration gradient and by inverse modelling.

2.2 Estimation of local advection fluxes from horizontal concentration gradients

In practice, the local advection flux (term (II) in Eq. 1)can be assessed with a simplified equation derived from Eq. (2), by assuming the integrand is constant with height, which then leads to the following relationship:

$$\Delta F_{z,\text{adv}}(x,z) = -(z - z_0) \cdot u(z) \cdot \frac{\partial \chi_a(x,z)}{\partial x} \tag{3}$$

Equation (3) was used in this study to estimate $\Delta F_{z,\text{adv}}(x,z)$ using measured wind speed and horizontal concentration gradient at 1 m height. The roughness height z_0 estimated by micrometeorological methods was small and negligible when compared to z=1 m.

2.3 Advection errors estimated using backward dispersion modelling

An alternative approach to estimate advection errors is based on the use of a two dimensional (2-D) dispersion model to infer the sources from measured concentration at several locations. This provides a means to constrain the advection flux estimates, as well as a way to estimate the spatial evolution of the advection fluxes with more details than measurement-based estimates. The modelling approach is based on the use of the general superposition principle (Thomson, 1987; Raupach, 1989; Flesch et al., 2007; McGinn et al., 2007), which relates the concentration at a location (x,z), $\chi_a(x,z)$, to the source strength at another location (x_S, z_S), $S(x_S, z_S)$, with the use of a dispersion function $D(x, z/x_S, z_S)$ (in $s\,m^{-3}$):

$$\chi_a(x, z) = \chi_{bgd} + \int_{all x_S} S(x_S, z_S) D(x, z/x_S, z_S) dx_S \quad (4)$$

where χ_{bgd} is the background concentration, assumed to be constant with height. $D(x, z/x_S, z_S)$ was estimated using the Green's approach to solve the two-dimensional advection-diffusion equation, based on the assumptions of power law functions to describe the wind speed $u(z)$ and the vertical diffusivity $K_Z(z)$ profiles (Yeh and Huang, 1975; Huang, 1979). A description of the dispersion model and a discussion about its quality and defaults is given in Loubet et al. (2001). The combination of Eqs. (2) and (4) gives the advection flux $\Delta F_{z,\mathrm{adv}}(x, z)$ once the sources $S(x_S, z_S)$ and the dispersion matrix are known. Note that $\Delta F_{z,\mathrm{adv}}(x, z)$ is independent of χ_{bgd} since it is a function of $\partial \chi_a(x, z)/\partial x$. In this study, $S(x_S, z_S)$ was used as a fitting parameter to minimise the difference between measured and modelled concentration at several distances. The way $S(x_S, z_S)$ was determined (its location and heterogeneity), as well as the fitting procedure is detailed in the following sections.

3 Material and methods

3.1 Site description

The field site was a 12 ha experimental grassland located in the grounds of the Forschungsanstalt Landwirtschaft (FAL), Braunschweig, Germany (Fig. 1). Directly adjacent to the field are an experimental farm of the FAL and a station of the German Weather Service (Deutscher Wetterdienst). The Site is described in details in Sutton et al., 2008. The experiment lasted from the 22 May 2000 to the 15 June 2000, over a period when the field I was cut (29 May 2000), and then fertilised with 100 kg NH_3 ha^{-1} of calcium ammonium nitrate (5 June 2000).

The main source of NH_3 in the area was the set of farm buildings (Site 5 in Fig. 1), which was emitting throughout the experimental period; the main field, which was a strong source after fertilisation, and a grass field (Grass field II in Fig. 1), which was spread with liquid manure the 24 May 2000. Other fields which might have been small NH_3 sources (Fields III and IV) were not taken into account. The distance from west to east is referred to as x, whereas the distance from south to north is referred to as y, while height above ground is z. The distance between the downwind edge of the farm building area and the different sites were estimated as 230 m for Site 3, 610 m for Site 1 and 810 m for Site 2. Site 6 was used for measuring the background concentration. The farm buildings themselves occupy an area of approximately 180 m (E-W)×200–300 m (S-N). The size of the equivalent two-dimensional source was set to 180 m in the E-W direction. The estimated emission strength ranged between 6.0 ± 0.17 kg d^{-1} NH_3 (FIDES-2-D model) and 9.2 ± 0.7 kg d^{-1} NH_3 (Gaussian model). These estimates were 94% and 63% of what was obtained using emission factors from the German national inventory (9.6 kg d^{-1} NH_3) as shown in Hensen et al., 2008.

The local advection fluxes were estimated at Site 1 and Site 2, where vertical NH_3 fluxes and concentration were also measured and described in Milford et al., 2008. Three periods were considered: (1) before the cut (29 May 2000), when the main local source was the farm buildings and the grassland was a small sink, (2) after the cut but before the fertilisation (5 June 2000), when the main field and the farm buildings were both contributing to local advection, and (3) after fertilisation, when the field was the main contributor to local advection.

3.2 Micrometeorological measurements

Micrometeorological measurements were performed at Site 1 and Site 2. These included eddy covariance fluxes measurements, which gave the wind direction (W_d), the friction velocity (u^*), the Monin-Obukhov length (L), and the sensible and latent heat fluxes (H and LE respectively). Also measured were the air temperature (T_a) and relative humidity (RH), as well as the global and net radiation (S_t and R_n respectively).

All these data were measured with replication, which allowed a consensus micrometeorological database to be established for the whole experimental field. Using the measured fluxes, T_a, u and RH were estimated at a reference height of 1 m above d. In the modelling approach, u^* and L were filtered to consider only data where: $u^*>0.2\,\mathrm{m\,s^{-1}}$ and $|L|>5\,\mathrm{m}$.

3.3 Ammonia concentration and fluxes measurements

Sites where NH_3 concentration was monitored are shown in Fig. 1. There were three AMANDA analysers (Wyers et al., 1993) placed in N-S line at Site 3, which gave NH_3 concentration on a 30 min averaging period. At Site 1, NH_3 concentration was measured with two AMANDA gradient systems and a mini-WEDD system giving quarterly-hourly vertical NH_3 fluxes and concentration at 1 m height. Four REA systems were also set at Site 1, which gave the flux at a height of 2.1 m above ground. At Site 2 fluxes and concentration were measured with a single AMANDA gradient system at 1 m height. The background concentration (χ_{bgd}) was measured with an automatic batch denuder system (Keuken et al., 1988), located at 42 m height near the top of a tower (Site 6, located 950 m to the E-NE of Site 1). In addition, daily concentrations were measured in grassland Field II (Fig. 1) at 400–600 m to the N of the main field, as part of a long-term denuder monitoring. Since χ_{bgd} only started to be measured at Site 6 at 15:00 GMT 26 May, the background concentration before that date was assumed to be that at Site 2. This implies that advection errors are assumed to be zero at Site 2 before this time. Mean and standard deviation of the NH_3 concentration was estimated for Site 1 and Site 3 over the three measurement systems. The concentration at each site i is referred to as χ_i in the following. In order to control the different sites, an unknown standard aqueous NH_4^+ sample was passed through all the analysers.

Figure 2 shows that χ_{bgd} is usually close to the daily denuder measurements performed 400–600 m north of the field, except for the days immediately following the application of manure to grassland Field II (24 and 25 May 2000), and to a smaller extent during the following 10 days. On 24 and 25 May 2000, the main source influencing local advection errors was therefore assumed to be the grassland Field II rather than the farm. The difference between χ_{bgd} and χ_1 is consistent with the differences in field management. Indeed, almost no difference between χ_1 and χ_{bgd} is observed before the cut (occurring the 29 May 2000), a small enhancement in χ_1 is observed after the cut, while a much larger enhancement occurred after the fertilisation (5 June 2000), which lasted approximately six days.

3.4 Inferred advection error $\Delta F_{z,\mathrm{adv}}$ from measured horizontal concentration gradients

The first method to infer $\Delta F_{z,\mathrm{adv}}$ at Site 1 is based on Eq. (3). The horizontal gradient $\partial \chi_a(x,z)/\partial x$ was estimated, in a simple approach, as the slope of the regression line between χ_a and x from measurements at sites 1, 2 and 3, using 15-minute data. The wind speed measured at Site 1 at 1 m height was used in Eq. (3). Due to the location of these sites, two wind-sectors were selected $245<WD<285$, corresponding to westerly winds, and $65<WD<105$ corresponding to easterly winds. The advection error at 1 m height was either positive when the horizontal gradient was negative, indicating an advective plume coming from the farm, or positive when the concentration was enhanced over the field, due to local emission of NH_3 following fertilisation.

3.5 Inferred advection error $\Delta F_{z,\mathrm{adv}}$ using a dispersion modelling approach

On the basis of Eqs. (2) and (4), the advection error $\Delta F_{z,\mathrm{adv}}$ at 1 m height at Site 1 was estimated as the superposition of the advection error due to the farm and the advection error due to the experimental field itself. The FIDES-2-D model (Flux Interpretation by Dispersion and Exchange over Short-range, in 2 Dimensions) (Loubet et al., 2001) was used to infer the emission strength from the source (S_{src}), using χ_3 and χ_{bgd}. For modelling purposes, the farm source was considered to be infinitely long in y and 180 m wide in x, and located at x=230 m upwind of site 3 (III in Fig. 1). No NH_3 surface exchange was considered in the fields located between the farm and the Field I, unless otherwise stated. As FIDES-2-D applies to homogeneous fields, a single

z_0 and a single d was considered for the whole distance downwind from the source, which were either taken from the micrometeorological dataset when modelling advection errors from the field, or fixed to z_0=0.1 m and d=0.5 m when modelling advections errors from the farm, since taller canopies and heterogeneities were present between the farm and the field.

Using the FIDES-2-D model, the NH_3 surface flux S_{field} was estimated in the experimental field (Kleinkamp in Fig. 1) using χ_3 as χ_{bgd} to take account of the enhancement of concentration at the entry of the field due to farm emissions. Two hypotheses were compared: *(H1)* S_{field} was considered constant over the whole field, and *(H2)* the canopy compensation point concentration χ_c (e.g., Sutton et al., 1995) was considered constant over the whole field, which implies a non-homogeneous S_{field}. The second hypothesis *H2* is based upon the compensation point approach, which relates S_{field} to χ_c by the following relationship: $S_{\text{field}}=-(\chi_{\text{surf}}-\chi_c)/R_b$ where χ_{surf} is the concentration at z_0, and R_b is the canopy excess resistance, estimated using the expression of Garland (1977). Under *H1*, S_{field} was tuned in order for the modelled and measured concentration χ_1 to fit, whereas under *H2*, χ_c was tuned instead of S_{field}. Since FIDES-2-D is a 2-D model, the equivalent field size upwind of Site 1 was assumed to be equal to the fetch between the side of the field and Site 1 for a given wind direction.

4 Results

4.1 Concentration enhancement due to the farm and the experimental field

Figure 3 shows the concentration rose for Sites 1, 2, 3, and the background concentration, which is generally smaller than all other concentrations, apart from χ_2 in some cases. The latter situation is explained by the fact that the experimental field is a local sink, since χ_2 is measured near the ground whereas χ_{bgd} is measured at 42 m height. Fig. 3 shows clearly that there is a concentration enhancement at Site 3 during westerly winds before fertilisation. The concentration enhancement is the largest when Site 3 is downwind from the farm, which corresponds to wind directions 270–280±30 degrees.

After fertilisation χ_1 is larger than χ_{bgd}, which indicates an NH_3 emission from the experimental field. Figure 4 shows three typical measured horizontal gradients in χ_a during westerly winds, corresponding to the pre-cut, post-cut and post-fertilisation periods. A clear difference can be seen between each situation: during the pre-cut period the horizontal concentration gradient is negative whereas it is positive during the post-cut and post-fertilisation periods. After fertilisation, there is always a larger concentration at Site 1 than at Site 2 during westerly winds, which might be either due to an effect of the trees on the east of the experimental field (change in wind direction, enhanced turbulence, ...), or the inhomogeneity of the field as an NH_3 emission source.

Figure 4 also shows the modelled concentration using the FIDES-2-D model. It can be seen that the modelled concentration coincides with the measured concentration at Sites 3 and 1 since these concentrations were used to fit the model. The three examples in Fig. 4 illustrate that two sources of advection errors (the farm, and the field) combined to either a net positive (25 May) or net negative (2 and 7 June) advection error, corresponding to a negative or a positive horizontal concentration gradient, respectively (see Eqs. 2 and 3). Figure 4 also shows that the mean concentration values used to estimate the measured advection error $\Delta F_{z,\mathrm{adv}}$ on the base of a linear regression between measured concentration and the distance may lead to overestimation of the horizontal concentration gradient at Site 1 as compared to the modelled one. This is especially true for the field induced advection errors, and would occur where there are other causes of concentration differences across the field (e.g. field source strength not spatially constant).

4.2 Local advection at site 1

Figure 5 shows the time course of the measured flux, the measured advection error (Eq. 3), and the modelled advection error (the latter split into advection error due to the farm and advection error due to the field), for three days (27 May, 7 and 12 June) at Site 1. These days show three typical situations: (1) on the 27 May (pre-cut period), the field is a small sink and the positive advection error mainly originate from the farm source; (2) on the 7 June (post-fertilisation), the field is a strong NH_3 source and is therefore the main contributor to the advection error, which are negative in these cases; (3) the 12 June (later after fertilisation) is a mix of local advection due to a small field source and a farm source, which leads to a small but positive advection error.

In Fig. 5, as for the whole period, the measured advection error $\Delta F_{z,\mathrm{adv}}$ at 1 m height is systematically larger in magnitude than the modelled one. The contribution of the farm to $\Delta F_{z,\mathrm{adv}}$ at z=1 m at Site 1 is bounded between 5 and 21 ng NH_3 m^{-2} s^{-1}, and 0 and 8 ng NH_3 m^{-2} s^{-1} for the measured and modelled advection error, respectively (top of Fig. 5). The contribution from the field itself to advection errors is much more variable, since it is related to the field emissions, which vary from about −50 ng NH_3 m^{-2} s^{-1} before the cut to more than 3000 ng NH_3 m^{-2} s^{-1} after the fertilization. Maximum advection errors at z=1 m due to the field were down to −90 and −32 ng NH_3 m^{-2} s^{-1} on the 07 June, as estimated by measurement and model, respectively. The modelled $\Delta F_{z,\mathrm{adv}}$ at z=2 m is also shown in Fig. 5, for comparison, and is much better correlated with the measured advection error, especially on the 12 June. Advection errors from the field, estimated under hypotheses *H1* (constant surface flux) and *H2* (constant surface concentration) did not differ significantly (data not shown).

The measured $\Delta F_{z,\mathrm{adv}}$ at Site 1 could represent more than 100% of the flux at 1 m height when the flux from the field was small, typically before the cut. When the field emissions were strong the advection errors, although large in magnitude were usually smaller than 5% of the flux at 1 m, as for example on the 7 June where they reached a maximum of 5.3%.

5 Discussion

5.1 Comparison of modelled and measured advection errors

The Braunschweig experiment provided the opportunity to validate the inverse modelling approach developed by Loubet et al. (2001) to infer the advection errors, by comparing with the direct estimates of advection errors from the measured horizontal concentration gradient. Figure 5 shows that the agreement is very good between the measured $\Delta F_{z,\mathrm{adv}}$ at 1 m height and the modelled $\Delta F_{z,\mathrm{adv}}$ at 2 m height for the given days. Figure 6 shows a scatter plot of the modelled versus measured advection errors for the whole period. In this graph, the positive and negative advection fluxes have been split in order to distinguish between periods when the dominant advection flux was due to the farm or the field.

Figure 6 confirms that the agreement between the two methods is good if $\Delta F_{z,\mathrm{adv}}$ is estimated at 2 m height with FIDES-2-D. At z=1 m height, the model underestimate the measured $\Delta F_{z,\mathrm{adv}}$ by 60% (as estimated by a linear regression in Fig. 6). This underestimation is larger under stable conditions than unstable conditions (data not shown). Several arguments are discussed which may explain the observed differences between measured and modelled $\Delta F_{z,\mathrm{adv}}$ at 1 m height:

(A1) A first argument is that the measured $\Delta F_{z,\mathrm{adv}}$ is estimated by linear regression over the whole field, whereas the model gives an estimate precisely at Site 1. $\Delta F_{z,\mathrm{adv}}$, which is proportional to the horizontal concentration gradient, evolves with distance from the source as illustrated by Fig. 4, and Fig. 6 (difference between Site 1 and Site 6). Indeed, it can be seen in Fig. 4 that the modelled horizontal concentration gradient at Site 1 is smaller than the slope from Site 3 to Site 2, hence explaining why the modelled advection error at 1 m is always smaller than the measured one. One the base of Fig. 4, it can be argued that the “measured advection error” is however larger than the real advection error at Site 1, and that the modelled one may be a better estimate.

(A2) A second argument is that the FIDES-2-D model does not estimate correctly the advection errors from the farm, which may be due to several reasons: (A3-1) uncertainty in the input parameters ($z_0, d, h_{srce}, \ldots$); (A3-2) no lateral dispersion is taken into account (the maximum underestimation of $\Delta F_{z,\mathrm{adv}}$ due to the farm at Site 1 was evaluated to be 100%; data not shown); *(A3-3)* no deposition upwind of the field is taken into account, which leads to underestimation of $\Delta F_{z,\mathrm{adv}}$ by a maximum of 50% (sensitivity analysis not shown);

(A3) A third argument is that the assumption of constant integrand in Eq. (2) to evaluate the measured $\Delta F_{z,\mathrm{adv}}$ in Eq. (3) does not hold. However, assuming logarithmic profiles for $u(z)$ and $\chi_a(z)$ (neutral conditions), shows that the estimate of Eq. (3) is equal to $2/\ln(z/z_0)$ times the exact integral of Eq. (2). With z_0=0.1 m and z=1 m, $2/\ln(z/z_0)$=0.87. Taking into account the logarithmic profiles of $u(z)$ and $\chi_a(z)$ would tend to increase further the measured $\Delta F_{z,\mathrm{adv}}$. Hence this argument can not explain the observed difference.

Out of these arguments it is difficult to draw definitive conclusions on the verification of the FIDES-2-D model. However, it seems that argument (A1) can explain part of the difference between the measured and the modelled $\Delta F_{z,\mathrm{adv}}$. Indeed, in Fig. 4 one sees that the horizontal concentration profile is not linear but rather logarithmic. Using a logarithmic regression rather than a linear one, leads roughly to a 30% reduction in the measured advection error at Site 1. Argument (A2) is also a possible explanation, since both lateral dispersion and deposition upwind of the field would increase the modelled $\Delta F_{z,\mathrm{adv}}$. Argument (A3) does not seem to hold, although under non-neutral conditions, the profile shape of the integrand of Eq. (2) may differ. This approach also recognizes the uncertainty in measuring absolute values of χ_a between instruments.

5.2 Magnitude of advection errors

Using estimates of the advection errors discussed in the previous section allows drawing a general picture of the relative magnitude of $\Delta F_{z,\mathrm{adv}}$ in comparison with the vertical fluxes at Site 1 and Site 2 at 1 m height. Table 1 shows the median and range of the different advection errors at 1 m height, in comparison with the measured vertical flux at the same height and location for 4 periods typical of NH_3 fluxes in intensively managed grassland.

The median advection error due to farm emissions is rather constant at Site 1 (~2–3 ng NH_3 m^{-2} s^{-1} from model estimates; 10–16 ng NH_3 m^{-2} s^{-1} from measurements), which is a consequence of the farm NH_3 source being rather constant over the campaign, albeit with a clear diurnal pattern (Hensen et al., 2008). However, before the cut, the measured advection error due to the farm represented 121% of the flux (median of absolute ratio). This proportion reduced to 14% during the post-cut period and was less than 6% after fertilisation. Since $\Delta F_{z,\mathrm{adv}}$ due to the farm is always positive, and since it is associated with a negative concentration gradient in the horizontal (Eq. 3), NH_3 deposition fluxes are underestimated, and, conversely emissions are over-estimated by the percentage given above. The magnitude of the advection error from the farm diminishes with distance: Site 1 is at 610 m from the downwind edge of the farm. At Site 2 (810 m downwind of the farm), the modelled advection errors due to the farm are on average 60% smaller than at Site 1. The advection error due to the field itself is directly linked with the actual surface flux, which makes it a rather constant fraction of about 1.5% of F_z(Site 1). In magnitude this can however represent quite a large flux (measured $\Delta F_{z,\mathrm{adv}}$ up to −90 ng NH_3 m^{-2} s^{-1}, the 07 June).

This study as well as Loubet et al. (2001) and Milford et al. (2001b) show that advection errors can represent a large fraction of the flux (more than 100%) when measuring small NH_3 fluxes at distance typically smaller than 400 m downwind of intensive sources such as farms and intensively grazed fields. Advection errors due to the field on which measurements are performed is usually not taken into account, except through a fetch limitation threshold. For heterogeneous sources and sinks like NH_3 (Dragosits et al., 1998), N_2O (Laville et al., 1999), but also water vapour above watered crops under arid climate (Itier et al., 1994), these advection errors may be large, especially if the fetch is smaller than the one encountered here. To illustrate this discussion, Fig. 7 shows the decrease of the modelled advection error due to both the farm and the field as a function of the fetch for the same three typical runs as in Fig. 4 (pre-cut, post-cut, and post-fertilisation). It can be seen that the local advection error at 1 m height represents the largest fraction of F_Z at a fetch of approximately 30 m, and then it decreases downwards. At x=100 m the advection error ranges between 3% and 15% of the flux and at x=200 m it ranges from 1.5% to 8% of the flux at 1 m. Further sensitivity analysis with FIDES-2-D (not detailed here) has shown that the distance at which the advection error at 1 m is maximum and the rate of decrease both depend upon the stability, but not much on u^*. With stable conditions, the advection error at 1 m height increases up to 300% of its value in neutral conditions, whereas in unstable conditions it diminishes to 50% of its value at neutrality.

5.3 The FIDES-2-D model as an independent method to infer NH_3 fluxes

The FIDES-2-D model (Loubet et al., 2001) has been adapted here to account for both the farm NH_3 emissions and the NH_3 fluxes above the experimental field. This paper focuses on modelled advection flux divergence due to advection. However, another notable result is that, in the process of estimating the advection errors due to the field, the FIDES-2-D model provides an alternative estimate of the surface flux in the experimental field, in a similar way as presented by Sommer et al. (2005) This modelled flux can then be compared with the gradient and REA estimates (Milford et al., 2008; Hensen et al., 2008; Sutton et al., 2008). As shown in Fig. 8, the flux $F_Z\{1\,\mathrm{m}\}$ at Site 1 inferred with FIDES-2-D using only $u^*, z_0, d, L, \chi_1, \chi_{bgd}$ and the fetch, fits closely to the fluxes measured by the gradient method, as reported for the mean estimate of the flux (consensus estimate) and the alternative estimate (given for some days where there was particular uncertainty between instruments, Milford et al., 2008). In Fig. 8, the flux estimated by FIDES-2-D is estimated assuming a constant surface concentration. The flux estimated with a hypothesis of a constant surface flux is 3% higher (R^2=0.9998, n=2126) than with constant surface concentration.

Figure 8 is a notable result for at least two reasons: (1) the two methods are relatively independent since the gradient method uses the vertical gradient near the ground and the FIDES-2-D method uses the concentration difference between two locations (χ_1(1 m), χ_{bgd}(42 m)). (2) This suggests that, when the geometry of the source/sink can be identified, only one concentration measurement close to the ground (1 m height) and one concentration measurement in the background are necessary to infer the fluxes, knowing u^*, z_0, d and L. Note that all data need to be measured on a fine temporal scale (30 min–2 h). The FIDES inference method worked well when the field was itself the main local source of NH_3, therefore driving the concentration change above the field, as is shown in Fig. 2. In a situation where the concentration at 1 m is driven by background sources located further away, such as during the first week of experiment (upper graph of Fig. 8), the method employed here is much more uncertain. It would also probably be more difficult to achieve good results in situations where the background and the local concentration are close to each other, due to a larger relative uncertainty in the concentration measurements.

Nevertheless, Fig. 8 demonstrates the interest of such an inference method: The concentration measurement between an emitting field and a background does not require the same precision as needed in a gradient or a REA flux measurement. Moreover, in this study the inference method can be used to discriminate between the flux measurements methods. In the situations where the consensus and alternative fluxes do not agree, especially for days 3, 8 and 10 June, the FIDES-2-D estimate thus provides a valuable independent estimate. On the 3 June, the FIDES-2-D estimate of the flux matches closely to the consensus flux, whereas the on 8 June it fits the alternative flux, and the 10 June it lays in between the two. Hence this comparison can be useful in interpreting the gradient flux measurements, such as for comparison with process based-model estimates (Burkhard et al., 2008; Personne et al., 2008; Sutton et al., 2008).

6 Conclusions

The divergences in the vertical NH_3 flux at 1 m height due to advection over an intensively managed grassland have been inferred from and inverse modelling approach and from direct measurements of the horizontal concentration gradients. The advection errors over the experimental field have been shown to result from the combination of advection due to farm emissions and due to emissions from the study field itself. A simple method consisting in adding up these advection fluxes in the model resulted in a combined local advection error, which was smaller than the measured advection error. A study of the possible arguments explaining the disagreement between the two methods indicated several possible sources of error, but suggested that the measured advection error was representative of the advection error at 2 m height rather than at 1 m height.

The advection error due to the farm emissions was positive, and ranged between approximately 0 and 27 ng NH_3 m^{-2} s^{-1}, at 610 m downwind, and was independent of the field fluxes. Relative to the flux at Site 1 after cutting and fertilisation, advection error due to the farm was small, but it represented 121% on average before the cut for periods when Site 1 was downwind of the farm. The field-induced advection errors were negative and represented a small fraction of about 1.5% of the flux on average but up to 7% punctually.

Therefore, advection errors, when using standard micrometeorological methods to measure emissions over an agricultural field, could lead to a systematic underestimation of NH_3 emissions to the atmosphere of up to 7%. Conversely, advection errors induced from point source such as a farm, over semi-natural land are not proportional to the flux, but depend on the farm source magnitude. This study shows that the magnitude of advection errors at 1 to 2 m height, resulting from point sources is likely to be about 10 ng NH_3 m^{-2} s^{-1} as an order of magnitude at 600 m downwind of an intensive source, but can reach hundreds of ng NH_3 m^{-2} s^{-1} at 300 m downwind from the farm. This means that in a regional budget, emissions from intensively managed fields would be underestimated and deposition to semi-natural areas would also be underestimated (Loubet et al., 2001; Milford et al., 2001b). Only where horizontal NH_3 concentration profiles are measured, or the source location can be identified and the difference from background NH_3 concentration is known, can these errors be determined and appropriate corrections made to the surface flux estimates. The results of this study provide advection corrections for flux measurements (Milford et al., 2008) as well as an independent estimate of the net flux for the GRAMINAE Braunschweig Experiment (Sutton et al., 2008).

Acknowledgements. The work presented here was partly funded by the EU GRAMINAE Project (contract ENV4-CT98-0722), the French Ministry of Research and Education, the French Ministry of Agriculture, the UK Department of Environment Food and Rural Affairs (Air and Environmental Quality Programme), the UK Natural Environment Research Council, and the FAL, Braunschweig. Final synthesis of this paper was conducted as part of the NitroEurope Integrated Project.

References

Bouwman, A. F., Lee, D. S., Asman, W. A. H., Dentener, J. F., van de Hoek, K. W., and Olivier, J. J. G.: A global emission inventory for ammonia, Global. Biogeochem. Cy., 11, 561–587, 1997.

Brost, R. A., Delany, A. C., and Huebert, B. J.: Numerical modeling of concentrations and fluxes of HNO_3, NH_3, and NH_4NO_3 near the surface, J. Geophys. Res., 93, 7137–7152, 1988.

Burkhardt, J., Flechard, C. R., Gresens, F., Mattsson, M. E., Jongejan, P. A. C., Erisman, J. W., Weidinger, T., Meszaros, R., Nemitz, E., and Sutton, M. A.: Modeling the dynamic chemical interactions of atmospheric ammonia and other trace gases with measured leaf surface wetness in a managed grassland canopy, Biogeosciences Discuss., 5, 2505–2539, 2008, http://www.biogeosciences-discuss.net/5/2505/2008/.

Itier, B., Brunet, Y., McAneney, K. J., and Lagouarde, J. P.: Downwind evolution of scalar fluxes and surface resistance under conditions of local advection.Part I: a rappraisal of boundary conditions, Agr. Forest. Meteorol., 71, 211–225, 1994.

Dragosits, U. Sutton, M. A., Place, C. J., and Bayley, A.: Modelling the spatial distribution of ammonia emissions in the UK, Environ. Pollut., 102(S1), 195–203, 1998.
Erisman, J. W., and Wyers, G. P.: Continuous measurements of surface exchange of SO_2 and NH_3: implications for their possible interaction in the deposition process, Atmos. Environ., 27A, 1937–1949, 1993.
Fangmeier, A., Hadwiger-Fangmeier, A., van der Eerden, L., and Jaeger, H. J.: Effects of atmospheric ammonia on vegetation – a review, Environ. Pollut., 86, 43–82, 1994.
Flesch, T. K., Wilson, J. D., Harper, L. A., Todd, R. W., and Cole, N. A.: Agr. Forest. Meteorol., 144, 139–155, 2007.
Foken, T., Wimmer, F., Mauder, M., Thomas, C., and Liebethal, C.: Some aspects of the energy balance closure problem, Atmos. Chem. Phys., 6, 4395–4402, 2006, http://www.atmos-chem-phys.net/6/4395/2006/.
Fowler, D., Coyle, M., Flechard, C., Hargreaves, K. J., Nemitz, E., Storeton-West, R., Sutton, M. A., and Erisman, J. W.: Advances in micrometeorological methods for the measurement and interpretation of gas and particle nitrogen fluxes, Plant Soil., 228(1), 117–129, 2001.
Fowler, D. and Duyzer, J. H.: Micrometeorological techniques for the measurement of trace gas exchange. in Exchange of Trace Gases Between Terrestrial Ecosystems and the Atmosphere, edited by: Andreae, M. O. and Schimel, D. S., 189–207, John Wiley, New York, 1989.
Garland, J. A.: The dry deposition of sulphur dioxide to land and water surfaces, Proc. R. Soc. Lon. Ser.-A., 354, 245–268, 1977.
Hensen, A., Nemitz, E., Flynn, M. J., Blatter, A., Jones, S. K., Sørensen, L. L., Hensen, B., Pryor, S., Jensen, B., Otjes, R. P., Cobussen, J., Loubet, B., Erisman, J. W., Gallagher, M. W., Neftel, A., and Sutton, M. A.: Inter-comparison of ammonia fluxes obtained using the relaxed eddy accumulation technique, Biogeosciences Discuss., 5, 3965–4000, 2008, http://www.biogeosciences-discuss.net/5/3965/2008/.
Hensen, A., Loubet, B., Mosquera, J., van den Bulk, W. C. M., Erisman, J. W., Dämmgen, U., Milford, C., Löpmeier, F. J., Cellier, P., Mikuska, P., and Sutton, M. A.: Estimation of NH_3 emissions from a naturally ventilated livestock farm using local-scale atmospheric dispersion modelling, Biogeosciences Discuss., submitted,, 2008.
Hertel, O., Skjøth, C. A., Lofstrøm, P., Geels, C., Frohn, L. M., Ellermann, T., and Madsen, P. V.: Modelling nitrogen deposition on a local scale – A review of the current state of the art, Environ. Chem. 3, 317–337, 2006.

Huang, C. H.: A theory of dispersion in turbulent shear flow, Atmos. Environ. 13, 453–463, 1979.

Kaimal, J. C. and Finnigan, J. J.: Atmospheric Boundary Layer Flows, Their Structure and Measurement. Oxford Univ. Press, New York, 1994.

Keuken, M. P., Schoonebeek, C., van Wensveen-Louter, A., and Slanina, J.: Simultaneous sampling of NH_3, HNO_3, HCl, SO_2 and H_2O_2 by a wet annular denuder system, Atmos. Environ., 22, 2541–2548, 1988.

Krupa, S. V.: Effects of atmospheric ammonia (NH_3) on terrestrial vegetation: a review, Environ. Pollut., 124, 179–221, 2003.

Laville, P., Jambert, C., Cellier, P., and Delmas, R.: Measurements of nitrous oxide fluxes in a fertilised maize crop by micrometeorological and chamber methods, Agr. Forest. Meteorol., 96, 19–38, 1999.

Lee, X.H., Yu, Q., Sun, X., Liu, J., Min, Q., Liu, Y., and Zhang, X.: Micrometeorological fluxes under the influence of regional and local advection: a revisit, Agr. Forest. Meteorol., 122(1/2), 111–124, 2004.

Leuning, R., Freney, J. R., Denmead, O. T., and Simpson, J. R.: A sampler for measuring atmospheric ammonia flux, Atmos. Environ., 19, 1117–1124, 1985.

Loubet, B., Milford, C., Sutton, M. A., and Cellier, P.: Investigation of the interaction between sources and sinks of atmospheric ammonia in an upland landscape using a simplified dispersion-exchange model, J. Geophys. Res., 106(D20), 24183–24198, 2001.

Loubet, B., Cellier, P., Milford, C., and Sutton, M. A.: A coupled dispersion and exchange model for short-range dry deposition of atmospheric ammonia, Q. J. Roy. Meteor. Soc., 132, 1733–1763, 2006.

McGinn, S. M., Flesch, T. K., Crenna, B. P., Beauchernin, K. A., and Coates, T.: Quantifying ammonia emissions from a cattle feedlot using a dispersion model, J. Environ. Qual., 36, 1585–1590, 2007.

Milford, C., Theobald, M. R., Nemitz, E., and Sutton, M. A.: Dynamics of ammonia exchange in response to cutting and fertilising in an intensively-managed grassland, Water, Air and Soil Pollution: Focus., 1(5–6), 167–176, 2001a.

Milford, C., Hargreaves, K. J., Sutton, M. A., Loubet, B., and Cellier, P.: Fluxes of NH_3 and CO_2 over upland moorland in the vicinity of agricultural land, J. Geophys. Res.-Atmos., 106(D20), 24169–24181, 2001b.

Milford, C., Theobald, M. R., Nemitz, E., Hargreaves, K. J., Horvath, L., Raso, J., Dämmgen, U., Neftel, A., Jones, S. K., Hensen, A., Loubet, B., Cellier, P., and Sutton, M. A.: Ammonia fluxes in relation to cutting and fertilization of an intensively managed grassland derived from an inter-comparison of gradient measurements, Biogeosciences Discuss., 5, 4699–4744, 2008, http://www.biogeosciences-discuss.net/5/4699/2008/.

Nemitz, E., Sutton, M. A., Fowler, D., Choularton, T. W., and Gallagher, M. W.: Modelling the size-dependent concentration and flux profiles of NH_4NO_3 aerosol modified by gas-to-particle conversion of NH_3 and HNO_3. In: Proceedings of EUROTRAC Symposium 96', vol 1, edited by: Borrell, P. M., Borrell, P., Kelly K., and Seiler W., Computational Mechanics Publications, Southampton, 205–210, 1997.

Nemitz, E., Sutton, M. A., Wyers, G. P., Otjes, R., Schjoerring, J. K., Gallagher, M. W., Parrington, J., Fowler, D., and Choularton, T. W.: Surface atmosphere exchange and chemical interaction of gases and aerosols over oilseed rape, Agr. Forest. Meteorol., 105, 427–445, 2000.

Nemitz, E. and Sutton, M. A.: Gas-particle conversions above a Dutch heathland: III. Modelling of size-dependent NH_4^+ fluxes as modified by the NH_3-HNO_3-NH_4NO_3 equilibrium, Atmos. Chem. Phys., 4, 1025–1045, 2004, http://www.atmos-chem-phys.net/4/1025/2004/.

Nemitz, E., Dorsey, J. R., Flynn, M. J., Gallagher, M. W., Hensen, A., Owen, S., Dämmgen, U., and Sutton, M. A.: Aerosol fluxes and gas-to-particle conversion above grassland following the application of NH_4NO_3 fertilizer, Biogeosciences Discuss., in preparation, 2008.

Nemitz, E., Hargreaves, K. J., Neftel, A., Loubet, B., Cellier, P., Dorsey, J. R., Flynn, M., Hensen, A., Weidinger, T., Meszaros, R., Horvath, L., Fruehauf, C., Sutton, M. A., and Gallagher, M. W.: Inter-comparison of measurements and assessment of the turbulent exchange and energy balance of an intensively managed grassland, Biogeosciences Discuss., in preparation, 2008.

Personne, E., Loubet, B., Herrmann, B., Mattsson, M. E., Schjoerring, J. K., Nemitz, E., Sutton, M. A., and Cellier, P.: SURFATM-NH_3: a model combining the surface energy balance and the bi-directional exchanges of ammonia at the field scale, Biogeosciences Discuss., accepted, 2008.

Raupach, M. R.: Stand overstorey processes, Philos. T. Roy. Soc. B. 324, 175–190, 1989.

Sommer, S. G., Genermont, S., Cellier, P., Hutchings, N. J., Olesen, J. E., and Morvan, T.: Processes controlling ammonia emission from livestock slurry in the field, Eur. J. Agron.,

BGD

6, 163–196, 2009

19(4), 465–486, 2003.
Sommer, S. G., McGinn, S. M., and Flesch, T. K.: Simple use of the backwards Lagrangian stochastic dispersion technique for measuring ammonia emission from small field-plots, Eur. J. Agron., 23, 1–7, 2005.
Sutton, M. A., Milford, C., Nemitz, E., Theobald, M. R., Hill, P. W., Fowler, D., Schjoerring, J. K., Mattsson, M. E., Nielsen, K. H., Husted, S., Erisman, J. W., Otjes, R., Hensen, A., Cellier, P., Loubet, B., David, M., Genermont, S., Neftel, A., Blatter, A., Hermann, B., Jones, S. K., Horvath, L., Führer, E., Mantzanas, K., Koukoura, Z., Gallagher, M., Williams, P., and Riedo, M.: Biosphere-atmosphere interactions of ammonia with grasslands: experimental strategy and results from a new European initiative, Plant Soil., 228, 131–145, 2001.
Sutton, M. A., Fowler, D., and Moncrieff, J. B.: The exchange of atmospheric ammonia with vegetated surfaces. I: Unfertilized vegetation, Q. J. Roy. Meteor. Soc., 119, 1023–1045, 1993.
Sutton, M. A., Schjoerring, J. K., and Wyers, G. P.: Plant – atmosphere exchange of ammonia, Philos. T. Roy. Soc. A., 351, 261–275, 1995.
Sutton, M. A., Milford, C., Dragosits, U., Place, C. J., Singles, R. J., Smith, R. I., Pitcairn, C. E. R., Fowler, D., Hill, J., ApSimon, H. M., Ross, C., Hill, R., Jarvis, S. C., Pain, B. F., Phillips, V. C., Harrison, R., Moss, D., Webb, J., Espenhahn, S. E., Lee, D. S., Hornung M., Ullyett, J., Bull, K. R., Emmett, B. A., Lowe, J., and Wyers, G. P.: Dispersion, deposition and impacts of atmospheric ammonia: Quantifying local budgets and spatial variability, Environ. Pollut., 102, 349–361, 1998.
Sutton, M. A., Erisman, J.-W. E., Dentener, F., and Möller, D.: Ammonia in the environment: From ancient times to the present, Environ. Pollut., 156, 583–604, 2008.
Sutton, M. A., Nemitz, E., Theobald, M. R., Milford, C., Dorsey, J. R., Gallagher, M. W., Hensen, A., Jongejan, P. A. C., Erisman, J. W., Mattsson, M. E., Schjoerring, J. K., Cellier, P., Loubet, B., Roche, R., Neftel, A., Herrmann, B., Jones, S. K., Lehman, B. E., Horvath, L., Weidinger, T., Rajkai, K., Burkhardt, J., Löpmeier, F. J., and Dämmgen, U.: Dynamics of ammonia exchange with cut grassland: Strategy and implementation of the GRAMINAE Integrated Experiment, Biogeosciences Discuss., submitted, 2008.
Sutton, M. A., Campbell, C., Milford, C., Mattsson, M. E., Schjoerring, J. K., Herrmann, B., and Riedo, M.: Application of a coupled grassland – gas exchange model to investigate the interactions between grassland management and ammonia fluxes. Biogeosciences Discuss., submitted, 2008.
Sutton, M. A., Nemitz, E., Milford, C., Erisman, J. W., Hensen, A., Cellier, P., David, M., Loubet,

B., Personne, E., Schjoerring, J. K., Mattsson, M. E., Dorsey, J., Gallagher, M., Horvath, L., Weidinger, T., Dämmgen, U., Neftel, A., Herrmann, B., Lehman, B., and Burkhardt J.: Dynamics of ammonia exchange with cut grassland: Synthesis of results and conclusions, Biogeosciences Discuss., submitted, 2008.

Thomson, D. J.: Criteria for the selection of stochastic models of particle trajectories in turbulent flows, J. Fluid Mech., 180, 529–556, 1987.

Van der Eerden, L. J. M., de Visser, P. H. B., and van Djik, C. J.: Risk of damage to crops in the direct neighbourhood of ammonia sources, Environ. Pollut., 102(S1), 49–53, 1998.

Walker, J. T., Robarge, W. P., Wuc, Y., and Meyers, T. P.: Measurement of bi-directional ammonia fluxes over soybean using the modified Bowen-ratio technique, Agr. Forest. Meteorol., 138, 54–68, 2006.

Walker, J., Spence, P., Kimbrough, S., and Robarge, W.: Inferential model estimates of ammonia dry deposition in the vicinity of a swine production facility, Atmospheric Environment Agricultural Air Quality: State of the Science (AAQ-2006), 42(14), 3407–3418, 2008.

Wichink Kruit, R. J., van Pul, W. A. J., Otjes, R. P., Hofschreuder, P., Jacobs, A. F. G., and Holtstag A. A. M.: ammonia fluxes and derived canopy compensation points over non-fertilized agricultural grassland in The Netherlands using the new gradient ammonia-high accuracy-monitor (GRAHAM), Atmos. Environ. 41, 1275–1287, 2007.

Wilson, J. D., Catchpoole, V. R., Denmead, O. T., and Thurtell, G. W.: Verification of a simple micrometeorological method for estimating the rate of gaseous mass transfer from the ground to the atmosphere, Agr. Meteorol., 29, 183–189, 1983.

Whitehead, J. D., Twigg, M., Famulari, D., Nemitz, E., Sutton, M. A., Gallagher, M. W., and Fowler, D.: Evaluation of laser absorption spectroscopic techniques for eddy covariance flux measurements of ammonia, Environ. Sci. Technol., 42(6), 2041–2046, 2008.

Wyers, G. P., Otjes, R. P., and Slanina, J.: A continuous-flow denuder for the measurement of ambient concentrations and surface-exchange fluxes of ammonia, Atmos. Environ., 27A(13), 2085–2090, 1993.

Yeh, G. T. and Huang, C. H.: Three-dimensional air pollutant modeling in the lower atmosphere, Bound.-Lay. Meteorol., 9, 381–390, 1975.

Table 1. Relative contribution to advection error from the farm and the experimental field during 4 periods: the pre-cut (22 May–29 May), post-cut (29 May–5 June), post-fertilisation (5 June–11 June) and 7 days after fertilisation (11 June–16 June) period. F_z(Site 1) is the measured vertical flux at z=1 m at Site 1, $\Delta F_{z,\mathrm{adv}}\{\mathrm{meas}\}$ is the measured advection error using Eq. (3), $\Delta F_{z,\mathrm{adv}}\{\mathrm{farm}\}$ and $\Delta F_{z,\mathrm{adv}}\{\mathrm{field}\}$ are the modelled advection errors at z=1 m due to the farm and the experimental field respectively. Also given is the median of the absolute value of the percentage of advection error for each contribution relative to F_z(Site 1).

Period	F_z(Site 1) ng NH_3 m^{-2} s−1		$\Delta F_{z,\mathrm{adv}}\{\mathrm{meas}\}$ ng NH_3 m^{-2} s−1		$\Delta F_{z,\mathrm{adv}}\{\mathrm{farm}\}$ ng NH_3 m^{-2} s−1		$\Delta F_{z,\mathrm{adv}}\{\mathrm{field}\}$ ng NH_3 m^{-2} s−1		$\lvert\Delta F_{z,\mathrm{adv}}\rvert/F_z$(Site1) % of F_z(Site 1)		
									meas	farm	field
Pre-cut	−4	[−57 ; 51]	16	[−1 ; 41]	2.8	[0.2 ; 26.6]	0.0	[−10.4 ; 8.8]	121%	32%	6.8%
Post-cut	61	[−106 ; 641]	13	[−2 ; 51]	2.2	[−0.4 ; 8.5]	−0.4	[−187 ; 21]	14%	3%	3.7%
Post-fert.	430	[1 ; 3638]	−2	[−89 ; 37]	2.5	[−2.3 ; 8.8]	−4.8	[−209 ; 13]	3.7%	0.7%	1.5%
7 d later	91	[−6 ; 571]	10	[−3 ; 58]	3.4	[−1.7 ; 10.7]	0.1	[−24 ; 35]	5.8%	1.5%	1.6%

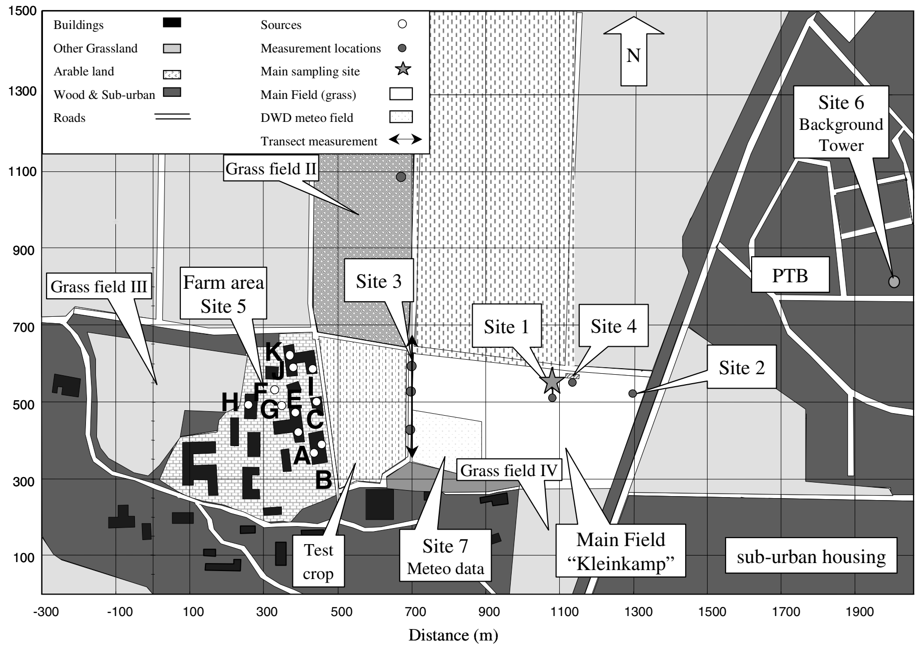

Fig. 1. Overview of the measurement site. The four concentration measurement locations used in this study are Site 1, Site 2 , Site 3, as well as Site 6 where the background concentration was measured. The NH_3 source buildings are detailed elsewhere. Main Field is field I, and grass field II is the field where slurry was spread the 24 May 2000.

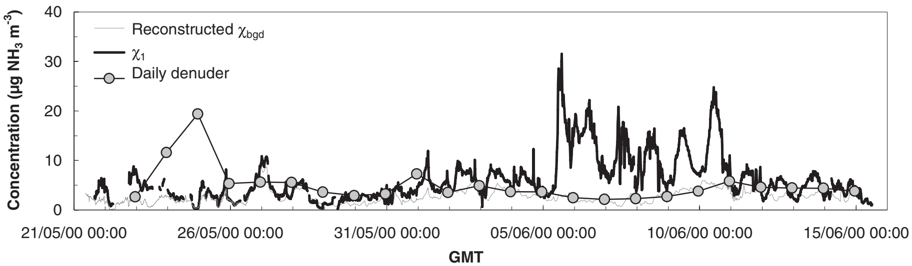

Fig. 2. Background concentration (χ_{bgd}) as measured with a batch denuder at Site 6 (800 m E-NE of Site 1), at 42 m height, compared with a daily denuder at grass field II (400–600 m N of Site 3), and the concentration at site 1 (χ_1). Since before the 15:00 GMT 26 May the background concentration was not available, and was reconstructed using the concentration at Site 2 (810 m downwind from the farm).

BGD
6, 163–196, 2009

Title Page
Abstract | Introduction
Conclusions | References
Tables | Figures
◀| |▶
◀ ▶
Back | Close
Full Screen / Esc
Printer-friendly Version
Interactive Discussion

BGD

6, 163–196, 2009

Local advection of NH_3 over a pasture field

B. Loubet et al.

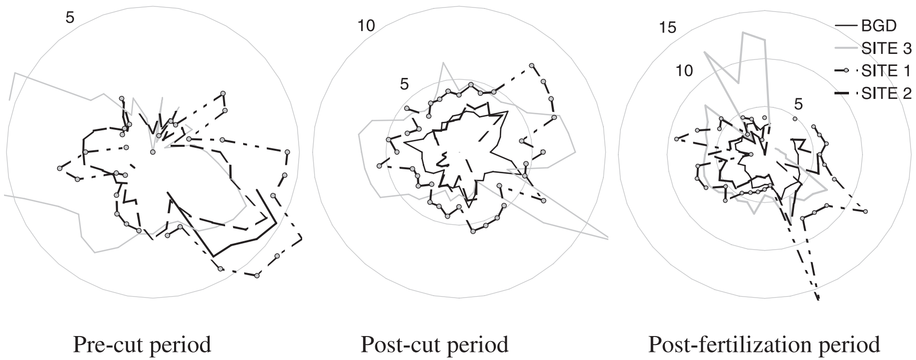

Fig. 3. Concentration rose, where NH_3 concentration at Sites 1, 2 and 3 as well as the background concentration (Site 6) is shown. The concentration rose has been calculated with quarterly hourly data, averaged over wind sectors of 10 degrees. All data have been averaged over three common periods: before the cut on the left, after cut in the middle, and after fertilisation on the right.

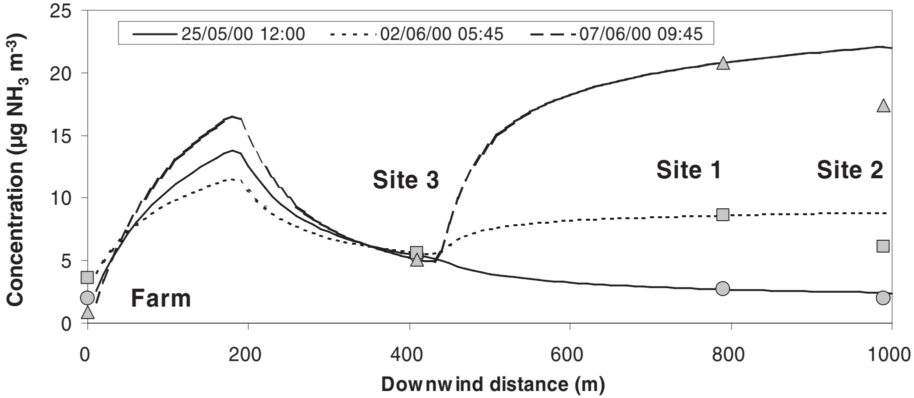

Fig. 4. Example horizontal gradient of measured NH_3 concentration at sites 1, 2 and 3, compared with the FIDES-2-D outputs. Three example runs are shown covering the pre-cut (12:00 GMT 25 May 2000, circles), post-cut (05:45 GMT 2 June 2000, squares) and post-fertilisation periods (09:45 GMT 7 June 2000, triangles), with similar NH_3 concentration at Site 3. These examples correspond to similar micrometeorological conditions (u^* and L). The model is given with lines whereas the measurements are shown with symbols. The measured concentrations shown at zero distance (upwind of the source) are those for χ_{bgd}.

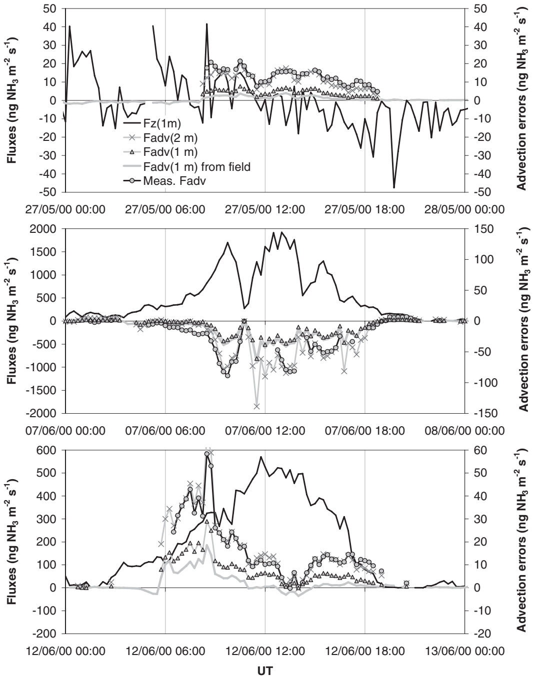

Fig. 5. Advection error ($\Delta F_{z,\mathrm{adv}}$) at 1 m and 2 m height for three typical days, before the cut (27 May 2000), just after fertilisation (7 June 2000) and a week after fertilization (12 June 2000). "Fz" is the measured flux at Site 1, "Meas. Fadv" is the measured local advection error, "Fadv" is the modelled local advection error at 1 m and 2 m, including the contribution from the field and the farm, and "Fadv (1 m) from field" is the local advection error due to field only. The advection errors can either be positive or negative, depending on the contribution of the field and the farm (see Fig. 4). Note the different y-scales. The advection errors from the farm are only given for periods when the wind was blowing from the farm.

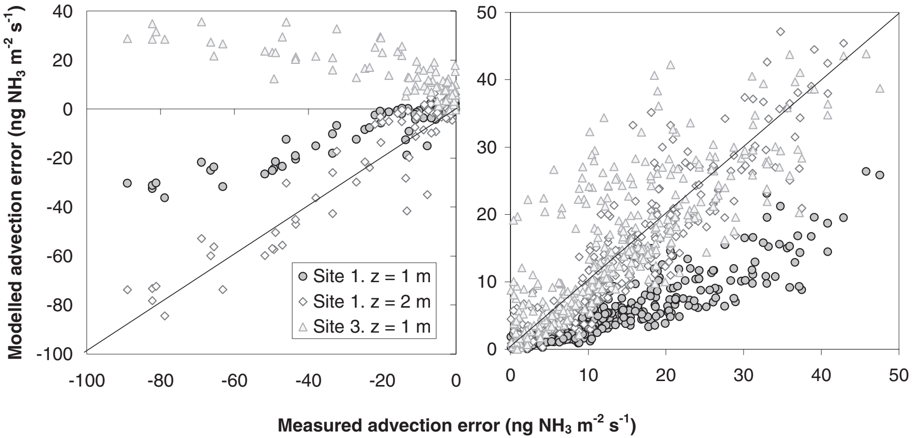

Fig. 6. Advection error ($\Delta F_{z,\mathrm{adv}}$) at z=1 m Site 1 (*circles*) and Site 3 (*triangles*), and at z=2 m at Site 1 (*diamonds*) estimated with the FIDES model, compared with ($\Delta F_{z,\mathrm{adv}}$) as estimated from the measured horizontal NH_3 concentration gradient over Sites 1, 2 and 3. The positive and negative modelled fluxes have been split to separate advection mainly due to the field (negative $\Delta F_{z,\mathrm{adv}}$) from advection mainly due to the farm buildings (positive $\Delta F_{z,\mathrm{adv}}$). A linear regression for the negative and positive modelled $\Delta F_{z,\mathrm{adv}}$ at Site 1 at z=1 m, gives $y=0.39x$ (R^2=0.86) and $y=0.40x$ (R^2=0.80), respectively (lines forced through 0). At z=2 m, the linear regression gives $y=0.93x$ (R^2=0.88) and $y=0.99x$ (R^2=0.86) for the negative and positive $\Delta F_{z,\mathrm{adv}}$, respectively. The data points correspond to wind blowing from the farm.

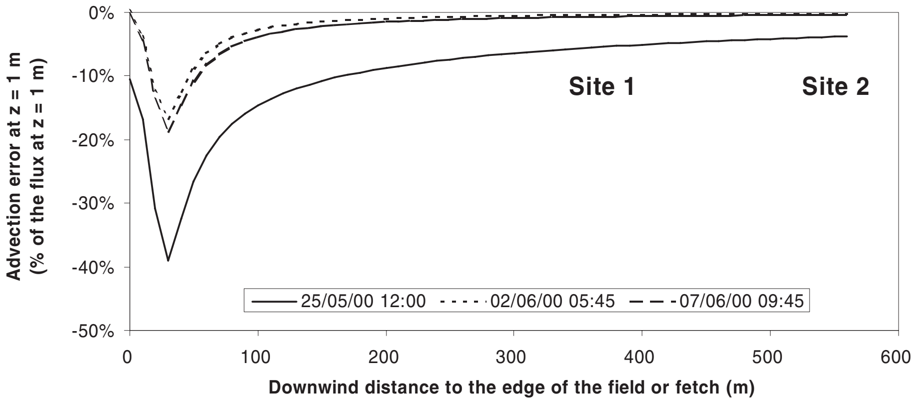

Fig. 7. Ratio of local advection error due to the field and the farm to flux at z=1 m, as a function of distance downwind of the edge of the field (fetch) for the same three runs as in Fig. 4, covering the pre-cut (25 May 2000 12:00, circles), post-cut (2 June 2000 05:45, squares) and post-fertilisation periods (7 June 2000 09:45, triangles), with similar NH_3 concentration at Site 3. Note that the ratio is always negative but the vertical flux was negative (deposition) the 25 May 12:00, whereas it was positive for the two other situations, while in the same time the local advection error was positive the 25 May and negative for the two other situations.

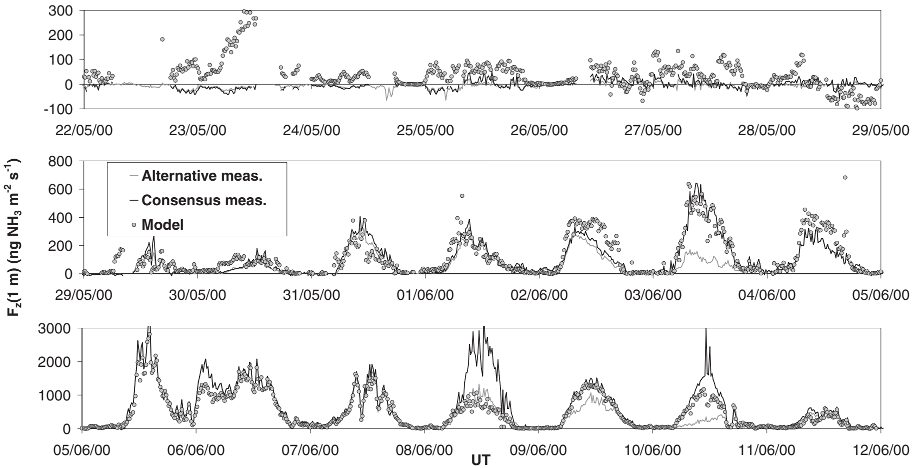

Fig. 8. Ammonia flux at z=1 m at Site 1 measured with the gradient technique (black line: consensus flux; grey line: Alternative estimate of the flux) and the FIDES-2-D surface dispersion model (diamonds) during the pre-cut period (upper graph), the pre-fertilisation period (middle graph), and the post-fertilisation period (bottom graph). The modelled flux has been inferred with the FIDES-2-D model using measured χ_1, χ_{bgd}, the fetch, as well as u^*, d, z_0, L. The consensus flux and the alternative estimate are detailed in Milford et al., 2008.